Lisa S. Egger*
Georg Fieg

Experimental Investigation of Decentralized Process Control for Reactive Dividing-Wall Columns

The reactive dividing-wall column (RDWC) presents a highly integrated process that enables significant reductions in investment costs and energy consumption. However, the high degree of integration of this apparatus causes numerous interactions between kinetics, vapor-liquid equilibrium, and mass transfer. To ensure a reliable operation of the RDWC, suitable control schemes need to be developed and experimentally validated. A decentralized control scheme for the RDWC is presented and for the first time experimentally investigated on an RDWC pilot plant. A comparison of experimental and simulated data is carried out and shows good agreement.

Supporting Information available online

Keywords: Distillation, Process control, Process integration, Reactive dividing-wall column

Received: November 19, 2019; *revised:* December 19, 2019; *accepted:* January 15, 2020

DOI: 10.1002/ceat.201900620

1 Introduction

Distillation is the most widely used separation technique in chemical industry. The high energy demand of this technology makes it responsible for a significant share of the global energy consumption. Volatile fuel costs as well as more and more strict environmental laws require the development of highly energy-efficient processes. The reactive dividing-wall column (RDWC) is a prime example for such an efficient process. By combining reactive distillation and dividing-wall column, the RDWC enables the production and separation of up to four product streams. It combines the advantages of the dividing-wall column like reduced energy demand for separation [1, 2] and the advantages of reactive distillation like higher conversion rates and selectivity [3, 4]. Weinfeld et al. call the RDWC an apparatus of second-level process integration [5] while Dejanović et al. [6] refer to the RDWC as "a step towards the ultimate sustainability in process industries". Simulation-based studies already showed a significant energy-saving potential compared to a sequence of reactive distillation and conventional distillation columns [7].

The growing number of published research articles in the past 15 years shows the increasing interest in RDWC technology. A comprehensive review of these works is presented by Weinfeld et al. [5]. Several experimentally validated steady-state models are available [8–10] and methods for an efficient column design have been developed [11, 12].

However, until today no industrial-scale application of the RDWC technology is known. From the industrial point of view a safe operation and stable product quality are essential for a successful implementation. While control concepts are available for reactive distillation [13, 14] and non-reactive dividing-wall columns [2, 15, 16], only little information is existing on the control of RDWCs. Most of the published works on RDWC control investigate the closed-loop behavior with mathematical models built in Aspen Dynamics [17–24]. Experimental data on the column's dynamic behavior are still scarce.

One recently published paper focuses on RDWC start-up [25]. However, experimental data on the performance of control schemes have not been published yet. Therefore, the aim of this work is to shed some light on the control of RDWCs in pilot-plant scale. First, a straightforward decentralized process control scheme is set up using a rigorous RDWC simulation model. Afterwards, the control scheme is tested in four different scenarios on an RDWC pilot plant and for the first time comprehensive experimental data on RDWC control are presented. As this work employs an integrated approach of modeling and experimental work to investigate the control of RDWCs, both simulation and experimental data are finally compared in a model validation.

2 Methodology

2.1 Pilot Plant

The transesterification of *n*-butyl acetate with 1-hexanol (Eq. (1)), catalyzed by the immobilized enzyme Novozym 435, is selected as reference system. A detailed investigation of the

Lisa S. Egger, Prof. Dr.-Ing. Georg Fieg
lisa.egger@tuhh.de
Hamburg University of Technology, Institute of Process and Plant Engineering, Am Schwarzenberg-Campus 4, 21073 Hamburg, Germany.

systems kinetics and binary phase equilibria was carried out in an earlier study [9]. The results indicate that the employment of Novozym 435 as catalyst enables a side product-free reaction. Two azeotropes occur at the investigated pressure range of 2–3 kPa. This allows the investigation of RDWC's successful operation and control even with non-deal phase behavior.

$$C_6H_{12}O_2 + C_6H_{14}O \rightleftharpoons C_4H_{10}O + C_8H_{16}O_2 \quad (1)$$

All presented experiments were conducted at the RDWC pilot plant of the Institute of Process and Plant Engineering at Hamburg University of Technology [9, 10, 25]. A picture of the pilot plant and a scheme that includes all sensors and base controllers (pressure and flow control) are displayed in Fig. 1. The column is 12 m high in total and built in a so-called Petlyuk configuration by spatial separation of prefractionator and main column. This configuration is thermodynamically equivalent to

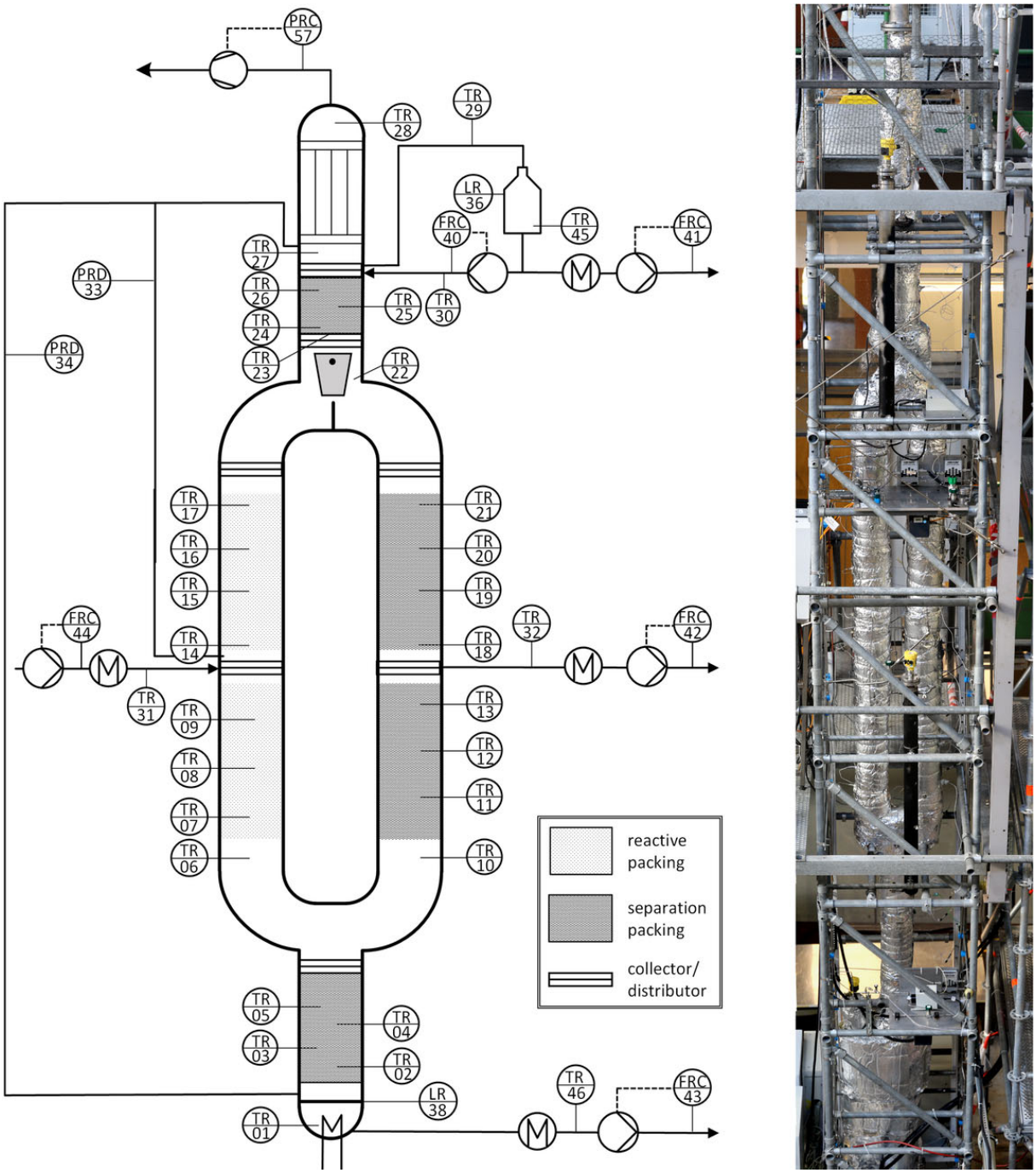

Figure 1. Picture (right) and scheme with available temperature and level sensors, flow and pressure controllers (left) of the RDWC pilot plant at Hamburg University of Technology.

an RDWC without heat transfer over the dividing wall. Thus, it emulates the behavior of industrial columns better, where the relative heat transfer is much smaller due to greater diameters in comparison to pilot plants.

As shown in Fig. 1, the column contains two reactive packing sections (DN 50), equipped with Katapak SP-Labor from Sulzer (two stages per meter), in the prefractionator and four non-reactive packing sections (DN 50 in dividing-wall section, DN 65 in upper and lower part), equipped with Montz B-500 structured packings (six stages per meter), in the main column. Each packing section has a height of 1 m. Thus, six theoretical stages are available each in the lower and the upper part of the column, four stages in the prefractionator, and twelve stages in the main column side of the dividing-wall section. A total of 280 g Novozym 435 is employed in the prefractionator. Liquid product samples are obtained from all three product streams. The analysis of liquid samples is carried out with a Clarus 500 gas chromatograph from Perkin Elmer with a Supelco SLB-5 column to determine the product concentrations.

For a detailed analysis of the RDWC dynamic behavior, the pilot plant is equipped with an extensive set of measuring devices, also indicated in Fig. 1. A total of 34 Pt100 temperature sensors (accuracy: $\pm(0.15 + 0.002T)$ °C), including four sensors at each packing segment, enable a high resolution of the temperature profile along the column. All incoming, i.e., feed and reflux, and outgoing, i.e., distillate, side and bottom, mass flows are measured by Coriolis mass flow meters (accuracy: $\pm 0.05\,\mathrm{kg\,h^{-1}}$). Additionally, the column top pressure (accuracy: $\pm 0.001p$ kPa), the pressure drop along the column (accuracy: $\pm 0.01p$ kPa), and the liquid levels (accuracy: ± 3 mm) in the distillate vessel and reboiler are measured.

2.2 Simulation Model

In order to predict the complex interactions of highly integrated processes like the RDWC, reliable dynamic process models are of particular importance. Furthermore, a precise model is the base for a successful implementation of advanced control schemes. In this work, a fully predictive dynamic RDWC model is presented that allows the simulation of the start-up, open-loop, and closed-loop column behavior. The model was developed at the Institute of Process and Plant Technology at the Hamburg University of Technology. A detailed description of the model assumptions and equations can be found in Egger and Fieg [25].

The model is set up in a modular structure. All model equations are solved with Aspen Custom Modeler (ACM). Property data are sourced via a link to Aspen Properties. The implemented modules include the RDWC column shell (divided into reactive and non-reactive sections and collector/distributers), the reboiler, the condenser, and the reflux drum. A scheme of the RDWC model with a description of all modules is presented in Fig. S1 in the Supporting Information. Process control is modeled by separate PID modules, provided by ACM, which allows for easy implementation of different control schemes.

The reboiler and RDWC column are modeled with the well-known equilibrium stage approach. Therefore, phase equilibrium (Eq. (2)) as well as mass and component balances are calculated (Eqs. (3) and (4)), taking into account the consumption and production of components by an additional reaction term, if a reaction is present. The Antoine equation is employed for calculation of vapor pressure of pure components, the UNIQUAC model is chosen for description of liquid phase non-idealities.

$$y_\mathrm{i} = K_\mathrm{i} x_\mathrm{i} \tag{2}$$

$$\frac{\mathrm{d}N}{\mathrm{d}t} = L_\mathrm{in} + V_\mathrm{in} - L_\mathrm{out} - V_\mathrm{out} + m_\mathrm{cat} \sum_{\mathrm{j}=1}^{\mathrm{n_R}} r_\mathrm{j} \tag{3}$$

$$\frac{\mathrm{d}Nx_\mathrm{i}}{\mathrm{d}t} = L_\mathrm{in} x_\mathrm{in,i} + V_\mathrm{in} y_\mathrm{in,i} - L_\mathrm{out} x_\mathrm{out,i} - V_\mathrm{out} y_\mathrm{out,i} + m_\mathrm{cat} \sum_{\mathrm{j}=1}^{\mathrm{n_R}} r_\mathrm{i,j} \tag{4}$$

The chemical reaction is modeled via a second-order power law approach as defined in Eqs. (5) and (6). The heat of reaction is taken into account by the heat of formation in the enthalpy balance (Eq. (7)). The enthalpy balance further includes two terms to model the effects of energy transfer to the stage's surroundings. The term Q_accu[1)] covers the heat transfer from each stage to the column steel shell. This term is especially relevant for strong changes of the column's temperature profiles, e.g., for start-up or disturbances. The term Q_loss describes the heat loss to the surroundings. Application of the summation conditions completes the well-known MESH equations.

$$r_\mathrm{j}(T) = k_\mathrm{j} \prod_{\mathrm{i}=1}^{\mathrm{n}} a_\mathrm{i} \tag{5}$$

$$k_\mathrm{j}(T) = k_\mathrm{0,j}\, e^{-\frac{E_\mathrm{A}}{R}\left(\frac{1}{T}-\frac{1}{T_0}\right)} \tag{6}$$

$$\frac{\mathrm{d}Nh}{\mathrm{d}t} = L_\mathrm{in} h_\mathrm{in,L} + V_\mathrm{in} h_\mathrm{in,V} - L_\mathrm{out} h_\mathrm{out,L} - V_\mathrm{out} h_\mathrm{out,V} - Q_\mathrm{loss} - Q_\mathrm{accu} \tag{7}$$

Finally, the vapor distribution in the dividing-wall section is addressed. Simulation studies proved the great influence of the vapor distribution on the energy efficiency of an RDWC [7, 12]. Therefore, a precise modeling of the vapor distribution, also called vapor split (VS), especially for the dynamic case is important. The vapor flow is automatically adjusted to ensure equal pressure drop on both sides of the dividing wall, i.e., main column (MC) and prefractionator (PF). The model emulates this effect through iterative solving Eqs. (8) and (9), where the pressure drop is calculated through an empirical correlation depending on the *f*-factor F_f, gas velocity u_L, axial length z, and empirical constants CP. The pressure drop modeling is described in detail by Ehlers et al. [10].

1) List of symbols at the end of the paper.

$$VS = 0.5 + K_{VS}\left(\Delta p^{MC} - \Delta p^{PF}\right) \quad (8)$$

$$\Delta p_i = CP_1 F_f^{CP_2}(1 + CP_3 u_L)\Delta z_i \quad (9)$$

2.3 Process Control Schemes

As no experimental data regarding process control of an RDWC have been published so far, a straightforward, relatively simple approach is selected to gain fundamental knowledge. Such a decentralized approach includes PI temperature, P-level and PI-pressure control loops. The column top pressure is controlled by a vacuum pump. All mass flows are controlled by flow controllers to ensure stable mass flows. Level and temperature controllers are operated in cascade mode.

The basic control scheme for the RDWC contains two level and two temperature controllers. Manipulated variables for level control are determined according to Richardson's rule. Since the reflux ratio is 4–12 for the considered experiments in this study, the reflux is chosen for level control of the reflux drum. The bottom stream is selected as manipulated variable for bottom level control. This leaves the distillate stream and the side stream for temperature control.

In this study, one temperature in the prefractionator and one temperature in the main column are to be controlled in order to ensure a constant conversion in the reactive zone and to manipulate the concentration profile in the main column, respectively. In this scheme, the heat duty is not yet applied as manipulated variable, in order to protect the enzymatic catalyst in the prefractionator. It was found in earlier studies [26] that the enzymatic catalyst is strongly deactivated by temperatures greater 60 °C. In the worst case, the enzymatic catalyst has to be exchanged, which takes several weeks, including assembly and time-consuming leakage tests of the apparatus. Therefore, for this first set of experiments the heat duty is purposely set to a fixed value that assures operation below 60 °C in the reactive zone. Based on the profound process knowledge gained in this study, the heat duty will be considered as manipulated variables in following studies.

In Fig. 2, a scheme with all possible configurations for temperature control loops as well as level, pressure, and flow control loops is presented. In order to find the exact temperature sensors that are suited as control variables and find a good pairing of control and manipulated variables, several analyses are conducted. First of all, the temperature slope and sensitivity are examined. Sensitivity analyses are conducted according to Kaymak and Luyben [27] by varying the manipulated variables by +1 %. Temperatures that are highly sensitive towards the change of manipulated variables are possible candidates as control variables. Afterwards, an SVD analysis and RGA are determined to decide the pairing of temperatures and manipulated variables.

Finally, the temperature controllers of each control scheme are tuned individually using the relay-feedback test. The obtained values may be slightly adjusted, based on the experience with the operation of the pilot plant, if the tuning is too aggressive. A slightly less aggressive tuning is desirable to prevent build-up of strong oscillations. Furthermore, temperature

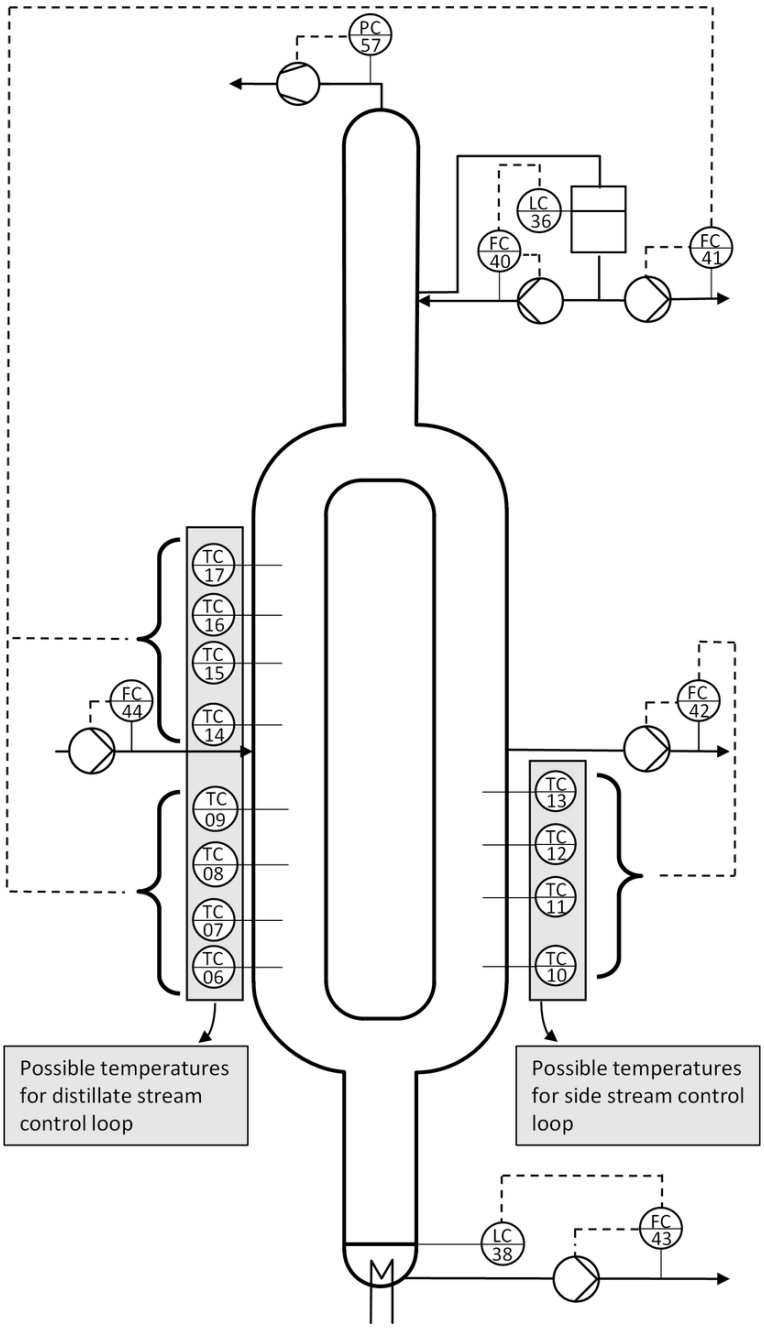

Figure 2. Control scheme of the RDWC pilot plant with all possible configurations for temperature control in the prefractionator and main column.

peaks are to be avoided in regards of the temperature-sensitive enzymatic catalyst. The process control scheme and the corresponding parameters are finally implemented into the distributed control system of the RDWC pilot plant.

3 Results

In order to investigate the control, two disturbance cases and two set point changes are examined. All experiments are also applied to validate the dynamic model presented in the prior section. In order to ensure the viability of the results for not only one operation point but different process conditions, a broad variety of different temperature and concentration profiles was chosen as starting points. The four different steady states which serve as starting points for the dynamic investigations are given in Tab. 1. The stationary values for heat duty and feed mass flow vary by more than 35 % and the butyl acetate mass fraction in the feed varies by more than 50 %. Fig. 3 displays the temperature profiles in the prefractionator and the main column of all four experiments. These operation points set the foundation for a thorough testing of the control system.

For every operation point a control scheme is set up according to the methodology described in Sect. 2.3. The results of the sensitivity analyses are given in Fig. S2 in the Supporting Information. The temperatures in the main column show high sensitivity towards both manipulated variables, the distillate, and the side stream, respectively. Therefore, some interactions between these two temperature control loops are expected. However, application of the SVD and RGA analyses helps to determine the final pairings. These pairings of selected temperature sensors and corresponding manipulated variables and the according tuning parameters are listed in Tab. 2 for all four operation points considered. Since level controllers remain unchanged, parameters are the same for all experiments.

For each experiment, the RDWC is run through the start-up phase, approx. 6–7 h, to achieve steady-state conditions. After approx. 2 h of steady-state operation, the disturbances and set point changes, respectively, are applied. In the first and fourth experiment, disturbances in the feed flow are examined. The second and third experiments examine the ability to perform set point changes. The forth experiment is chosen exemplarily to depict the model validation. An overview of the investigated scenarios is given in Tab. 3.

Table 1. Input parameters for steady-state conditions for all experiments.

		Exp. 1	Exp. 2	Exp. 3	Exp. 4
Reboiler duty [W]		920	860	860	1180
Liquid split [–]		0.35	0.45	0.35	0.35
Condenser pressure [kPa]		2.35	2.35	2.35	2.35
Reflux stream [kg h^{-1}]		5.12	4.8	4.90	7.42
Reflux ratio [–]		4.61	12	7.21	12.37
Feed stream [kg h^{-1}]		2.36	1.67	1.84	2.31
Feed composition [kg kg^{-1}]	Butyl acetate	0.676	0.418	0.675	0.533
	Hexanol	0.324	0.582	0.325	0.467
Distillate stream [kg h^{-1}]		1.11	0.4	0.68	0.60
Distillate composition [kg kg^{-1}]	Butyl acetate	0.798	0.805	0.803	0.803
	Butanol	0.202	0.205	0.197	0.197
Side stream [kg h^{-1}]		0.32	0.36	0.49	0.5
Side stream composition [kg kg^{-1}]	Butyl acetate	0.804	0.177	0.803	0.774
	Butanol	0.196	0.35	0.187	0.226
	Hexyl acetate	0	0.332	0.01	0.0
	Hexanol	0	0.141	0	0.0
Bottom stream [kg h^{-1}]		0.93	0.92	0.7	1.21
Bottom stream composition [kg kg^{-1}]	Butanol	0.03	0	0	0
	Hexyl acetate	0.601	0.278	0.528	0.371
	Hexanol	0.396	0.722	0.472	0.629

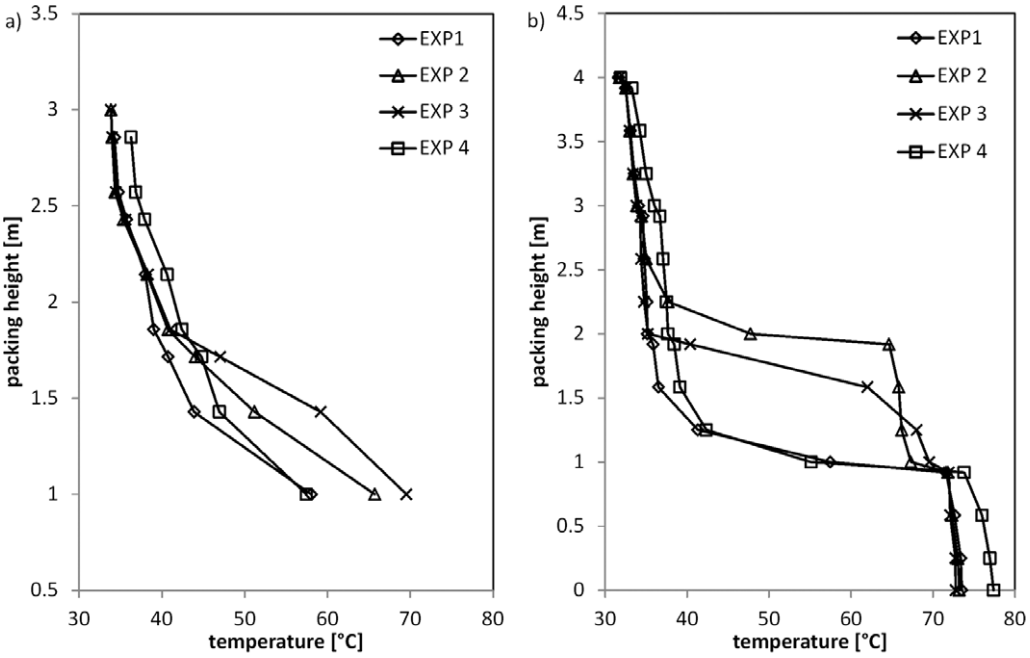

Figure 3. Temperature profiles in the prefractionator (a) and main column (b) of all four experiments.

Table 2. PI parameters of all controllers.

Exp.	Manipulated variable	Control variable	Gain [kg h^{-1}°C^{-1}] or [kg h^{-1}mm^{-1}]	Integral time [s]
1	Distillate stream F41	Temperature T06	0.1	745
	Side stream F42	Temperature T10	0.1	400
2	Distillate stream F41	Temperature T14	0.6	920
	Side stream F42	Temperature T11	0.2	100
3	Distillate stream F41	Temperature T14	0.5	745
	Side stream F42	Temperature T12	0.2	200
4	Distillate stream F41	Temperature T14	0.2	745
	Side stream F42	Temperature T11	0.1	400
1–4	Bottom stream F43	Reboiler level	0.06	–
	Reflux stream F40	Distillate vessel level	0.1	–

Table 3. Overview of investigated scenarios and objectives in this study.

Exp.	Objective	Variable	Magnitude of change of variable
1	Investigation of disturbance behavior	Feed mass flow	+20 %
2	Investigation of set point change behavior	Temperature T14 in prefractionator	+1 °C
3	Investigation of set point change behavior	Temperature T12 in main column	+4 °C
4	Model validation	Feed mass flow	–9 %

3.1 Experiment 1 – Feed Flow Disturbance

Disturbances in the feed flow are common disturbances that occur in industrial practice and that need to be handled by the process control scheme reliably. Therefore, the first scenario investigated is a disturbance in the feed mass flow by +20 %. The dynamic courses of the temperature control loop in the prefractionator and in the main column are illustrated in Fig. 4.

Prior to the introduction of the disturbance, both temperature and concentration profile are constant. The change in the feed flow immediately affects the temperature profile of the prefractionator and thus reactive zone as indicated in Fig. 4a. The controlled temperature T06 in the bottom of the reactive zone increases by 2 °C whereupon the distillate stream is decreased by over 20 %. After a slight undershoot of T06, the set point temperature of 58 °C is regained by the control loop. The side stream control loop is displayed in Fig. 4b. After a short rising of the controlled temperature T10, an undershoot follows before the temperature can be led back to the set point of 57.5 °C. The fast response of the control loop makes it possible to keep the composition of the product streams constant within a small deviation of max. 0.68 wt %. This is within measuring accuracy of the applied gas chromatograph. Exemplarily, the composition of the distillate stream is demonstrated in Fig. 5.

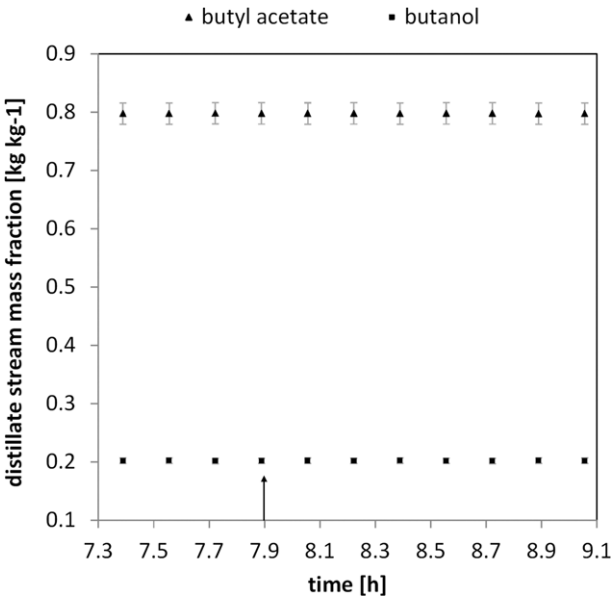

Figure 5. Composition of distillate stream after a disturbance of feed flow of +20 % at 7.9 h.

3.2 Experiments 2 and 3 – Set Point Changes

The ability of the control scheme to adjust new set points is an important feature that is needed when process conditions change, e.g., changes in feed composition or feed ratio. Fig. 6 presents two applied set point changes. In Fig. 6a, the set point for the controlled temperature in the prefractionator is increased by +1 °C, starting from steady-state conditions at 38 °C. The control loop induces a swift increase of the distillate stream by approx. 50 % in order to raise the temperature. This causes a slight overshoot of the temperature by approx. 0.5 °C. Within 1 h the desired set point is achieved.

In Fig. 6b, the set point for the controlled temperature in the main column is shown with the side stream. A set point change of 4 °C is induced. The side stream is increased to raise the temperature profile and then decreases gradually in order to keep the set point at the new obtained value. The adjustment time is considerably smaller than for the distillate stream control loop. Since the distance between side stream and T12 is relatively small compared to the distillate stream and T14, side stream adjustments directly affect the desired temperature without a significant lag time.

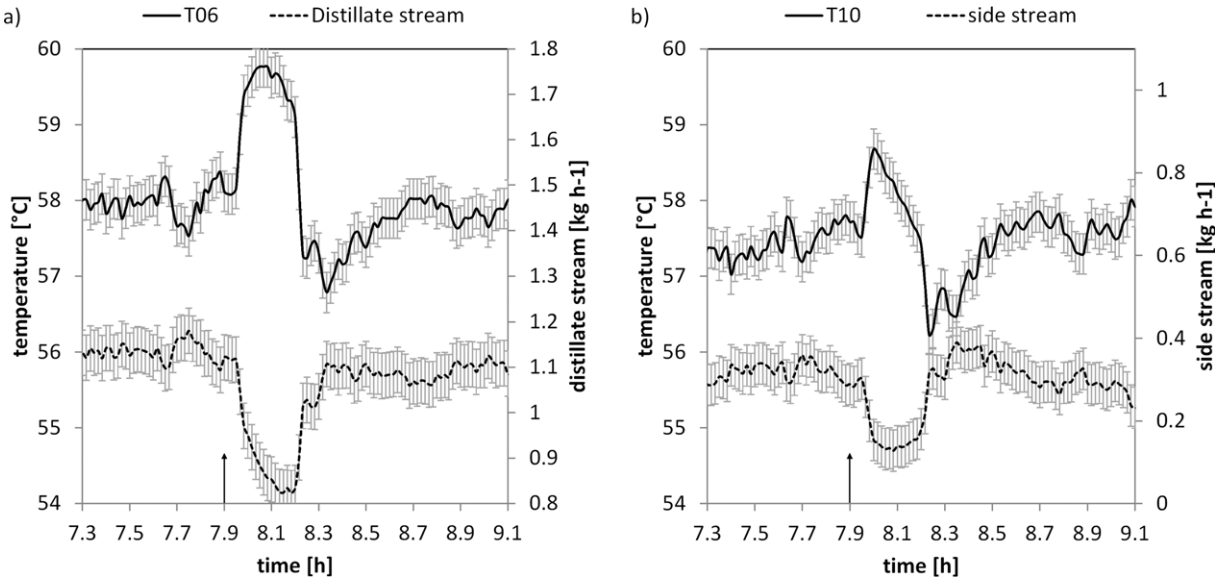

Figure 4. Disturbance of feed flow of +20 % at 7.9 h. (a) Measured values for controlled temperature T06 and distillate stream; (b) measured values for controlled temperature T10 and side stream.

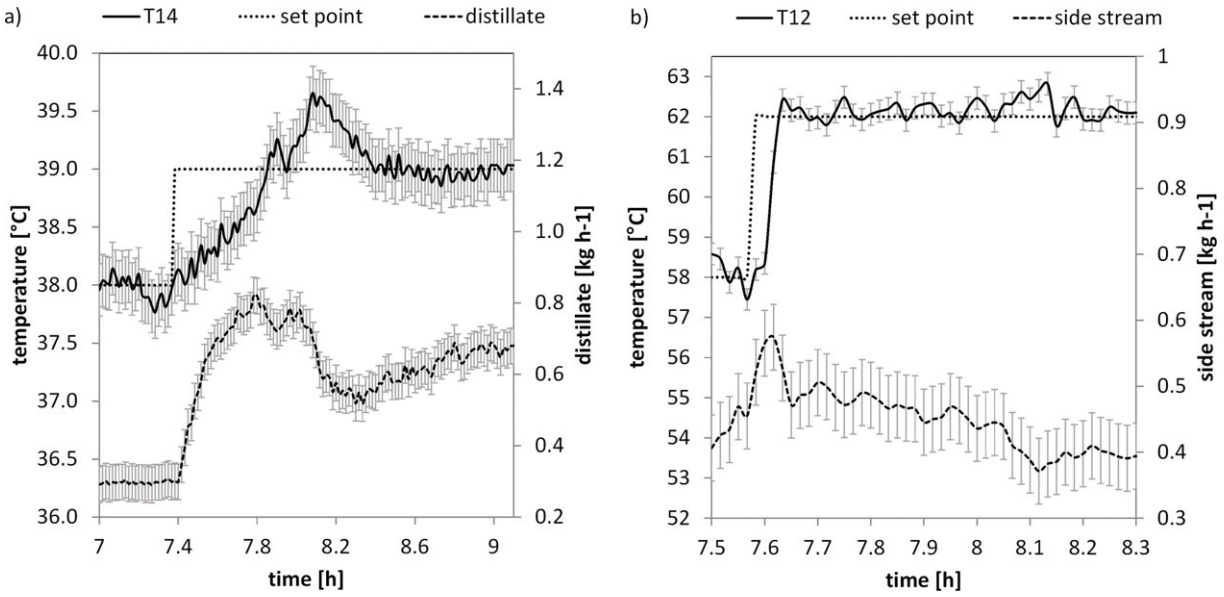

Figure 6. Dynamic courses of temperature control loops. (a) Set point change of +1 °C for T14 and corresponding distillate stream; (b) set point change of +4 °C for T12 and corresponding side stream.

3.3 Experiment 4 – Model Validation

Model validation is an essential step to verify simulation models and assure an accurate prediction of the dynamic RDWC behavior. Such validated models are the base for design of advanced control schemes. For the model described in Sect. 2.2, a validation was carried out by inserting steady-state as well as dynamic data, obtained at the pilot plant, into the simulation as input data. The predicted time courses of temperature and concentration are then compared to the experimental results. For the validation all four presented experiments were considered. Experiment no. 4 is exemplarily chosen to demonstrate the comparison of measured and simulated data in Fig. 7.

Fig. 7a presents the measured and simulated data of the distillate control loop and Fig. 7b depicts the composition of the distillate stream for feed mass flow disturbances applied at 7.8 h. As can be seen in both graphs, the simulated data fit the experimental values very well. Especially the dynamic courses of temperature and distillate stream are predicted with excellent accuracy. The validation of the concentration profile shows

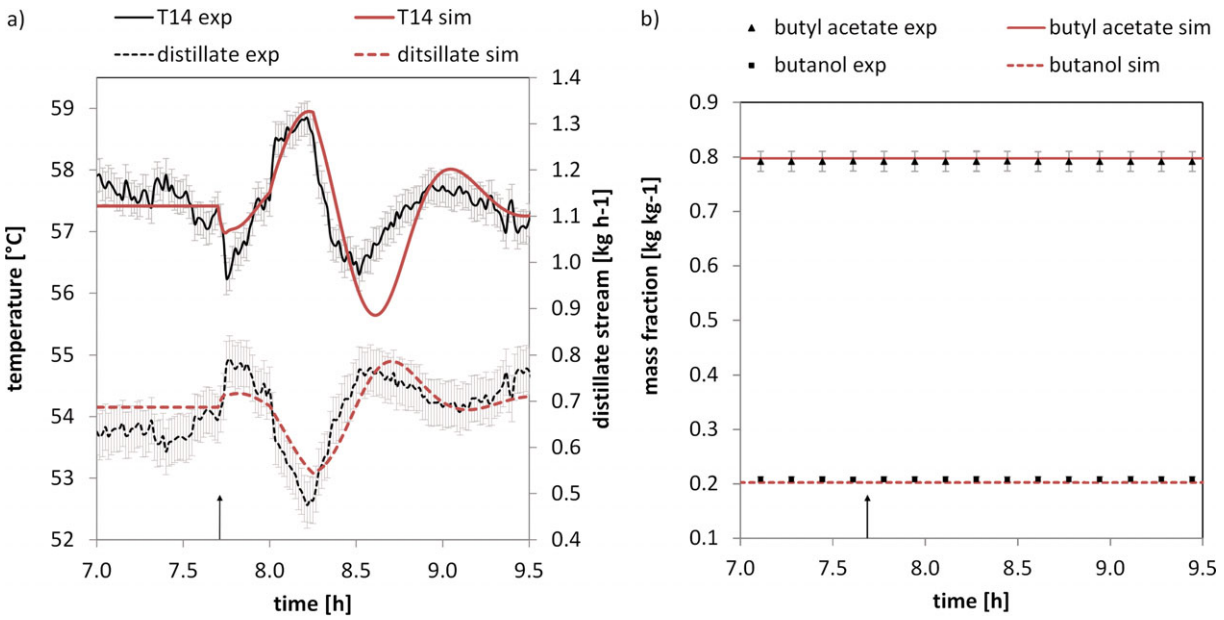

Figure 7. Comparison of measured (exp) and simulated (sim) data at a feed flow disturbances of –9 % at 7.8 h. (a) Controlled temperature T14 and distillate stream; (b) distillate stream composition.

a good agreement of experimental and simulation results. Furthermore, it can be seen that the control scheme is able to keep the concentrations constant throughout the disturbance.

4 Discussion and Conclusion

The RDWC was operated using a decentralized straightforward control scheme with two PI-temperature control loops. The applied disturbances and set point changes could be handled by the presented control scheme. However, in order to influence and control all key components in the three outlet streams, at least three temperature control loops should be applied. In the presented control scheme the heat duty was purposely operated at a fixed value. This approach was chosen because deactivation of the highly temperature-sensitive enzymatic catalyst was to be avoided at all costs. By conducting the presented experiments, valuable information about temperature changes in the reactive zone was obtained.

Four different operation points could successfully be investigated without danger of catalyst deactivation. Based on the fundamental understanding that was gained about the action and interactions of the temperature controllers in this study, the heat duty will be applied as manipulated variable in the future. Another manipulated variable that can be applied in the RDWC is the liquid split. It was found in simulation studies that the control of the liquid split is a promising technique in order to run the RDWC at energy-efficient operation [28]. However, a fourth control loop will also enhance the interactions in the column further and should only be applied if the dynamics of the system are well known. Taking into account the knowledge gained in this study, the liquid split will also be considered as manipulated variable in further studies with the RDWC pilot plant.

In conclusion, a well-tested and feasible control scheme is an essential step for a successful industrial application of the RDWC. This paper presents first comprehensive experimental data on RDWC control. The successful experimental test of the control scheme demonstrates that it is possible to maintain desired product purities even for significant feed mass flow disturbances as well as adjusting different set points. Testing the simulation model against hard experimental data shows a good prediction quality and thus gives valuable insights for the dynamic modeling of a complex system like the RDWC. By means of the validated dynamic model, more advanced process control schemes, both decentralized and centralized, can be designed for the operation of the RDWC pilot plant to further improve the control behavior.

The authors have declared no conflict of interest.

Symbols used

a_i	[–]	activity of component *i* in liquid phase
CP_1	[$kPa^{0.5}m^{-1}$]	constant for pressure drop calculation
CP_2	[–]	constant for pressure drop calculation
CP_3	[–]	constant for pressure drop calculation
E_A	[$J\,mol^{-1}$]	activation energy
F_f	[$Pa^{0.5}$]	*F*-factor
h	[$J\,mol^{-1}$]	molar enthalpy
k	[$mol\,s^{-1}kg^{-1}$]	temperature-dependent reaction rate constant
k_0	[$mol\,s^{-1}kg^{-1}$]	temperature-independent reaction rate constant
K_i	[$mol\,mol^{-1}$]	molar phase equilibrium constant
K_{VS}	[kPa^{-1}]	constant for vapor split calculation
L	[$mol\,s^{-1}$]	liquid molar flow
m_{cat}	[kg]	mass of Novozym 435 on a stage
N	[mol]	amount of moles
P	[kPa]	pressure
Δp^{MC}	[kPa]	pressure difference in main column
Δp^{PF}	[kPa]	pressure difference in prefractionator
Q_{loss}	[$J\,s^{-1}$]	heat loss to surroundings
Q_{accu}	[$J\,s^{-1}$]	heat accumulation in column internals and shell
R	[$J\,mol^{-1}K^{-1}$]	universal gas constant
r	[$mol\,s^{-1}kg^{-1}$]	reaction rate
T	[°C]	temperature
T_0	[K]	reference temperature for reaction kinetics
t	[s] or [h]	time
u_L	[$m\,s^{-1}$]	gas velocity
V	[$mol\,s^{-1}$]	molar vapor flow
x	[$kg\,kg^{-1}$]	liquid-phase molar fraction
y	[$kg\,kg^{-1}$]	vapor phase molar fraction
Δz	[m]	axial length

Sub- and superscripts

i	component index
in	inlet stream
j	stage index
L	liquid phase
out	outlet stream
Prod	product
Reac	reactant
V	vapor phase

Abbreviations

ACM	Aspen Custom Modeler
RDWC	reactive dividing-wall column
RGA	relative gain array
SVD	singular value decomposition
VS	vapor split

References

[1] K. Glinos, M. F. Malone, *Chem. Eng. Res. Des.* **1988**, *66*, 229–240.

[2] Ö. Yildirim, A. A. Kiss, E. Y. Kenig, *Sep. Purif. Technol.* **2011**, *80 (3)*, 403–417. DOI: https://doi.org/10.1016/j.seppur.2011.05.009
[3] *Integrated Reaction and Separation Operations: Modelling and Experimental Validation* (Eds.: H. Schmidt-Traub, A. Górak), Springer, Berlin **2006**.
[4] R. Taylor, R. Krishna, *Chem. Eng. Sci.* **2000**, *55 (22)*, 5183–5229. DOI: https://doi.org/10.1016/S0009-2509(00)00120-2
[5] J. A. Weinfeld, S. A. Owens, R. B. Eldridge, *Chem. Eng. Process.* **2018**, *123*, 20–33. DOI: https://doi.org/10.1016/j.cep.2017.10.019
[6] I. Dejanović, L. Matijašević, I. J. Halvorsen, S. Skogestad, H. Jansen, B. Kaibel, Ž. Olujić, *Chem. Eng. Res. Des.* **2011**, *89 (8)*, 1155–1167. DOI: https://doi.org/10.1016/j.cherd.2011.01.016
[7] M. Schröder, C. Ehlers, G. Fieg, *Chem. Eng. Technol.* **2016**, *39 (12)*, 2323–2338. DOI: https://doi.org/10.1002/ceat.201500722
[8] I. Müller, E. Y. Kenig, *Chem. Ing. Tech.* **2010**, *82 (12)*, 2109–2118. DOI: https://doi.org/10.1002/cite.201000084
[9] T. Egger, G. Fieg, *AIChE J.* **2017**, *53 (6)*, 2198–2211. DOI: https://doi.org/10.1002/aic.15598
[10] C. Ehlers, T. Egger, G. Fieg, *AIChE J.* **2017**, *63 (3)*, 1036–1050. DOI: https://doi.org/10.1002/aic.15435
[11] S.-J. Wang, D. S. H. Wong, S.-W. Yu, *Comput. Chem. Eng.* **2008**, *32 (12)*, 3030–3037. DOI: https://doi.org/10.1016/j.compchemeng.2008.04.001
[12] M. Schröder, G. Fieg, *Chem. Eng. Technol.* **2016**, *39 (12)*, 2265–2272. DOI: https://doi.org/10.1002/ceat.201600134
[13] *Reactive Distillation Design and Control* (Eds.: W. L. Luyben, C.-C. Yu), Wiley, Hoboken, NJ **2008**.
[14] *Reactive Distillation: Status and Future Directions* (Eds.: K. Sundmacher, A. Kienle), Wiley-VCH, Weinheim **2003**.
[15] C. Buck, C. Hiller, G. Fieg, *Chem. Eng. Process.* **2011**, *50 (2)*, 167–180. DOI: https://doi.org/10.1016/j.cep.2010.12.014
[16] C. Buck, C. Hiller, G. Fieg, *Chem. Eng. Technol.* **2011**, *34 (5)*, 663–672. DOI: https://doi.org/10.1002/ceat.201000487
[17] D. An, W. Cai, M. Xia, X. Zhang, F. Wang, *Chem. Eng. Process.* **2015**, *92*, 45–60. DOI: https://doi.org/10.1016/j.cep.2015.03.026
[18] X. Dai, Q. Ye, H. Yu, X. Suo, R. Li, *Ind. Eng. Chem. Res.* **2015**, *54 (15)*, 3919–3932. DOI: https://doi.org/10.1021/acs.iecr.5b00147
[19] S. Feng, Q. Ye, H. Xia, J. Chen, T. Liu, W. Wu, *Chem. Eng. Res. Des.* **2018**, *132*, 409–423. DOI: https://doi.org/10.1016/j.cherd.2018.01.026
[20] X. Qian, S. Jia, Y. Luo, X. Yuan, K.-T. Yu, *Chin. J. Chem. Eng.* **2016**, *24 (9)*, 1213–1228. DOI: https://doi.org/10.1016/j.cjche.2016.04.045
[21] X. Qian, S. Jia, S. Skogestad, X. Yuan, Y. Luo, *Ind. Eng. Chem. Res.* **2016**, *55 (36)*, 9738–9748. DOI: https://doi.org/10.1021/acs.iecr.6b02112
[22] S.-J. Wang, H.-P. Huang, C.-C. Yu, *Asia-Pac. J. Chem. Eng.* **2011**, *6 (3)*, 357–368. DOI: https://doi.org/10.1002/apj.569
[23] L. Li, L. Sun, D. Yang, W. Zhong, Y. Zhu, Y. Tian, *Chin. J. Chem. Eng.* **2016**, *24 (10)*, 1360–1368. DOI: https://doi.org/10.1016/j.cjche.2016.05.023
[24] L. Zheng, W. Cai, X. Zhang, Y. Wang, *Chem. Eng. Process.* **2017**, *111*, 127–140. DOI: https://doi.org/10.1016/j.cep.2016.09.014
[25] T. Egger, G. Fieg, *Chem. Eng. Sci.* **2018**, *179*, 284–295. DOI: https://doi.org/10.1016/j.ces.2017.12.011
[26] T. Egger, L. S. Egger, G. Fieg, *Chem. Eng. Sci.* **2018**, *178*, 324–334. DOI: https://doi.org/10.1016/j.ces.2017.12.050
[27] D. B. Kaymak, W. L. Luyben, *Ind. Eng. Chem. Res.* **2005**, *44 (13)*, 4625–4640. DOI: https://doi.org/10.1021/ie058012m
[28] L. S. Egger, G. Fieg, *Chem. Eng. Res. Des.* **2019**, *144*, 397–404. DOI: https://doi.org/10.1016/j.cherd.2019.02.026

